Time-resolved ion energy distribution functions in the afterglow of an EUV-induced plasma

Applied Physics Letters

Time-resolved ion energy distribution functions in the afterglow of an EUV-induced plasma

Cite as: Appl. Phys. Lett. **115**, 183502 (2019); https://doi.org/10.1063/1.5125739
Submitted: 26 August 2019 . Accepted: 23 September 2019 . Published Online: 30 October 2019

J. Beckers, T. H. M. van de Ven, and V. Y. Banine

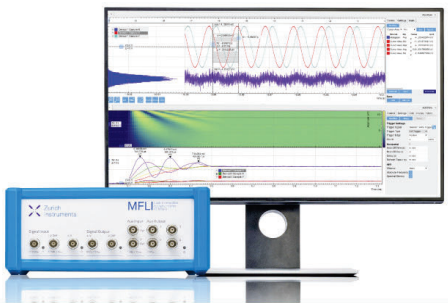

Applied Physics Letters ARTICLE scitation.org/journal/apl

Time-resolved ion energy distribution functions in the afterglow of an EUV-induced plasma

Cite as: Appl. Phys. Lett. **115**, 183502 (2019); doi: 10.1063/1.5125739
Submitted: 26 August 2019 · Accepted: 23 September 2019 ·
Published Online: 30 October 2019

J. Beckers,[1,a)] T. H. M. van de Ven,[1,2] and V. Y. Banine[1,2]

AFFILIATIONS

[1]Department of Applied Physics, Eindhoven University of Technology, 5612AP Eindhoven, The Netherlands
[2]ASML, 5504DR Veldhoven, The Netherlands

[a)]Author to whom correspondence should be addressed: j.beckers@tue.nl

ABSTRACT

Since the introduction of extreme ultraviolet (EUV) lithography (EUVL), the inevitable presence of EUV-induced plasmas inside the lithography tools impacts the operation of EUV optical components. EUV-induced plasmas are created everywhere in the optical path due to the ionizing interaction between the high energy (92 eV) EUV photons and the tools' background gas, which typically is hydrogen gas at a pressure of 1–10 Pa. From a physical point of view, the main impact of the plasma is due to the presence of ions that imping the plasma-facing surfaces. Experimental research into the fluence and energy distribution functions (IEDFs) of ions from EUV-induced plasmas has been limited to time-averaged measurements. In this Letter, we present time-resolved measurements of IEDFs for H^+, H_2^+, and H_3^+ ions from an EUV-induced plasma in pure hydrogen gas. To this end, an electrostatic quadrupole plasma (EQP) analyzer has been used. The measurements pinpointed momentary fluxes up to three orders of magnitude higher than earlier reported average ion fluxes. In addition, the mean ion energy was unexpectedly found to remain elevated up to 50 μs after the gas had been irradiated with EUV photons. Also, it was shown that the EQP detects H_2^+ ions on time scales much larger than expected. The presented results are valuable not only for the understanding of elementary processes regarding EUV-induced plasmas interacting with surfaces but also for simulating and predicting the impact of EUV-induced plasma on the lifetime and stability of optical components in EUVL.

With the introduction of extreme ultraviolet lithography (EUVL), i.e., lithography using 13.5 nm extreme ultraviolet (EUV) photons,[1] the industry and related scientific fields have shown major interest in EUV-induced plasmas; a peculiar type of plasma inevitably experienced during the operation of EUVL tools.[2] EUV-induced plasmas have been observed in the optical path of such tools[3] where they are the result of the ionizing interaction of the high energy photons (92 eV) with the low pressure (1–10 Pa) hydrogen (H_2) background gas. Since the photolithographic process is conducted in a repetitive manner, the induced pulsed plasma is highly transient with an initial electron energy distribution function (EEDF) that is non-Maxwellian. EUV-induced plasmas are recognized by the field to impact the long term operation of multilayer EUV optical components.[4–7] Optimization of the plasma conditions can lead to improvement of operation, e.g., in terms of cleaning EUV optical surfaces.[8–10]

Over the last few years, EUV-induced plasmas have been characterized from their optical emission[11–13] and from an electron dynamics point of view using numerical simulations[14,15] and experiments such as those using Langmuir probes[16,17] and microwave cavity resonance spectroscopy (MCRS) not only in H_2[18–21] but also in argon environments.[18,22–24] Also, the ionic components have been experimentally characterized using retarding field energy analyzers (RFEAs) and electrostatic quadrupole plasma (EQP) analyzers in pure H_2[25,26] and recently in H_2 diluted with a small fraction of nitrogen.[27] Until now, these measurements have always been time-averaged.

In this Letter, we present EQP measurements of species-resolved and energy-resolved ion energy distribution functions (IEDFs) for ions produced in EUV-induced plasmas in H_2, which are temporally resolved. As a complementary tool–not resolving ionic species but having a higher temporal resolution–an RFEA is used in addition to interpret and verify the findings. The results pinpoint momentary fluxes up to three orders of magnitude higher than earlier reported average ion fluxes and reveal some unexpected plasma physical features. As such, they are valuable not only for a better understanding of EUV-induced plasmas in general but also for modeling and predicting (long-term) impact of EUV-induced plasmas on EUV optical components in EUVL tools.

The used experimental configuration is similar to that in our previous works,[25,27] with the difference that the readout electronics of the

EQP device is slightly adapted to enable time-resolved measurements. Overall, the experimental setup consisted of three connected vacuum chambers (see Fig. 1). The source chamber housed a xenon-based discharge produced plasma (DPP) EUV source.[28] The collector chamber housed the "EUV collector" focusing the EUV radiation in the "focus" in the measurement chamber. The investigated EUV-induced plasma was created inside an aluminum measurement cylinder inside the measurement chamber and had an inner diameter and height of 100 mm. The shape and dimensions of this volume have been chosen for the purpose to optimize comparison with other experiments[19] and simulations.[14] The measurement cylinder contained a hole at its front surface to allow EUV radiation to enter. The back-end of the cylinder was closed by an aluminum end-plate concentrically containing the front-cap of the EQP device. Furthermore, the sidewall contained several pressure-balance holes and an opening to slide in and out a calorimetric power sensor being the same as previously used.[27,29]

The pulsed beam of EUV light had a repetition rate of 500 Hz, a full-width-at-half-maximum pulse duration of ∼50 ns (with a total pulse length of ∼100 ns), and a measured spectrum-integrated pulse energy of 121 ± 7 μJ at the position of the measurement cylinder. At the interface between the collector chamber and the measurement chamber, the radiation passes a 50 nm thick Si:Zr membrane, acting as an optical filter suppressing the out-of-band (>20 nm) radiation. This filter also ensures that fast ions generated by the EUV source cannot enter the measurement volume and influence the EUV-induced plasma dynamics. The EUV beam focused by the collector had its focal point exactly in the center of the measurement cylinder where the beam's diameter and convergence were 4 mm and 10°, respectively. At the position of the front-cap of the EQP, the beam's diameter was 32 mm, corresponding to a local EUV intensity of 283 W/cm^2, which is comparable with conditions in EUVL tools. Before and after each measurement, the stability and pulse energy of the EUV source were verified using the calorimetric power sensor.

The vacuum chambers were differentially pumped to ensure the independent control of the gas pressure in each of these chambers. In the measurement chamber, the base pressure was below 10^{-5} Pa. Pressure balance holes inside the walls of the measurement cylinder and feedback-controlled pumping speed and flow controllers assured a stable H_2 gas pressure of 5 Pa.

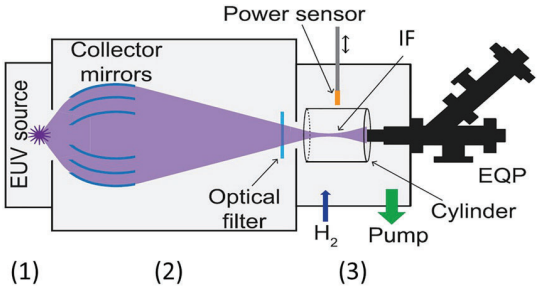

FIG. 1. Schematic overview of the experimental setup used (not to scale) with (1) the source chamber housing the EUV source, (2) the collector chamber housing the focusing optics and optical filter, and (3) the measurement chamber housing the measurement cylinder and the EQP diagnostics. Reproduced with permission from Beckers *et al.*, "Energy distribution functions for ions from pulsed EUV-induced plasmas in low pressure N_2-diluted H_2 gas," Appl. Phys. Lett. **114**(13), 133502 (2019). Copyright 2019 AIP Publishing.

The used EQP1000, Hiden analytical Ltd., and its application to EUV-induced plasmas with similar geometry and conditions are extensively discussed in our previous works.[25–27] Here, we suffice with only the main features.

The EQP1000 samples ions that enter the device through an orifice in its ruthenium-coated stainless steel front-cap, which in turn was sunken in the plasma-facing back-end closure of the measurement cylinder. An orifice diameter of 20 μm was chosen because it is sufficiently small compared to the Debye length (∼40 μm for typical values for the electron temperature (1 eV) and the electron density (3×10^{16} m^{-3}) in these kinds of plasmas[25]) to prevent plasma to enter and disturb the EQP. Before being detected by the secondary electron multiplier (SEM), which had a dynamic range of 7 orders of magnitude, the ions were energy and mass (range 1–50 amu) filtered by 15 individually adjustable electrostatic lenses inside the EQP (see Refs. 25 and 26 for the optimization of the lens settings). In essence, the EQP1000 was already equipped with the possibility to gate the detector relative to an externally provided trigger signal and hence able to measuring time-resolved. However, it would have taken several hours to map a plasma dynamic process of 2 ms (such as here) with microsecond resolution. To prevent issues with source stability on these timescales, a custom field programmable gate array (FPGA) multiscanner scaler was used to measure directly the output of the SEM ion detector. With that, the measurement time per setting was reduced by almost two orders of magnitude. Although the EQP contained an ion detector that was as fast as 50 ns, the bandwidth of the energy filter limited the overall time resolution to 5–10 μs (extensively explained in Ref. 26).

Figure 2 shows the temporal evolutions of IEDFs for H^+, H_2^+, and H_3^+ ions from the afterglow of a plasma induced by irradiating pure H_2 gas at 5 Pa (typical pressures used in EUVL tools) with a pulse (121 ± 7 μJ) of EUV-radiation.

These measurements indicate that the maximum momentary fluxes of roughly 10^7 c/s for H_3^+ (and 10^6 c/s for H^+ and H_3^+) are two to three orders of magnitude higher than the time-averaged values in similar plasma configurations reported in our earlier works.[25,27]

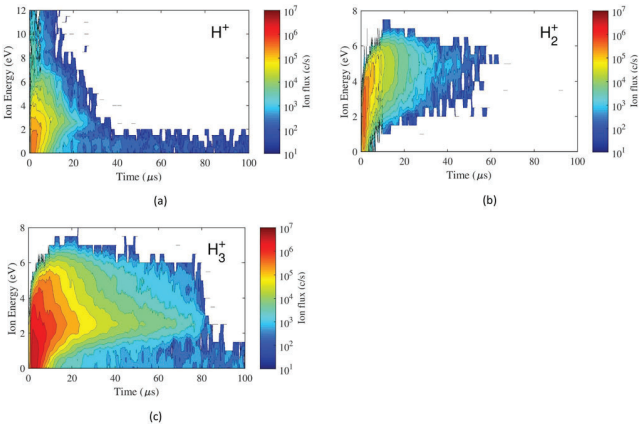

FIG. 2. Time-resolved IEDFs for (a) H^+, (b) H_2^+, and (c) H_3^+ from EUV-induced plasmas in pure H_2 gas at 5 Pa. The EUV pulse energy was 121 μJ. The shown data are averaged using a running average filter over 2 μs from 5 μs after gas irradiation onward for H^+ and from 10 μs after gas irradiation onward for both H_2^+ and H_3^+.

Furthermore, the shapes of the IEDFs establish over the first 5–10 μs after irradiation of the gas. This can—as discussed earlier and elaborated on in Ref. 26—be attributed to the limited temporal resolution of the EQP. The fact that this feature represents the time response of the EQP rather than "real" plasma dynamics is verified by temporally resolved measurements at identical configurations by an RFEA; see Fig. 3 where the shape of the energy distribution function (for all ions together) establishes at much shorter timescales. A detailed description of the RFEA and the manner in which it is applied to the EUV-induced plasmas in our configuration can be found in Ref. 25.

From a plasma dynamics point of view, the main results [Figs. 2(a)–2(c)] show two peculiarities.

I: Once the shapes of the IEDFs have developed, they remain roughly unaltered over the course of the plasma decay.

This is in contrast to what would be expected from earlier experiments mapping the electron dynamics in comparable decaying EUV-induced plasmas.[24,29] Considering that the energy of the incoming ions (into the EQP) is only determined by the potential drop over the developed space charge region (which in its turn is determined by the electron temperature), ion energies are expected to have decreased down to a few times room temperature within the first 1–10 μs. On this timescale, electron thermalization to room temperature was observed.[24,29] The measurements here, however, indicate elevated ion energies up to 50 μs after irradiation of the gas. Note that a similarly elevated ion mean energy (2 eV) was found in the late afterglow (600 μs after the plasma was switched off) of a pulsed inductively coupled hydrogen plasma by Osiac *et al.*[30]

II: H_2^+ is unexpectedly detected up to 50 μs in the afterglow phase.

This is in contrast to what would be expected when considering the highly efficient proton-hop collision reaction:

$$H_2^+ + H_2 \rightarrow H_3^+ + H. \quad (1)$$

This reaction has a very large cross section resulting from the (Langevin collision) mechanism where the H_2^+ ion induces a dipole moment in the H_2 molecule, leading to an attracting potential. The reaction in Eq. (1) has a rate constant of 2×10^{-9} cm^3 s^{-1},[31] which means in this case that H_2^+ created by photoionization during the EUV pulse will be converted into H_3^+ on time scales of 0.1–1 μs typically.

Starting with the observation of elevated mean ion energies, apparently, even after the irradiation of the H_2 has stopped, and thus no external energy was supplied to the system anymore, the temperature of the electrons remains high for a significantly longer time than expected. To give a first order approximation of the desired electron energy to explain observation I (ion energies of roughly 2.5–3 eV over the course of the plasma decay), we approximate the developed space charge region in front of the front-cap of the EQP as a traditional collisionless plasma sheath,[26] i.e., on these relatively long time scales, the afterglow of such an EUV-induced plasma can be approached as steady-state since the plasma's highly transient characteristics are present during the first 0.1–1 μs after initiation only. The potential drop Φ_w over the collisionless plasma sheath—over which the ions are accelerated to the front-cap of the EQP device—can be computed as[32]

$$\Phi_w = -T_e \ln\left(\frac{m_i}{2\pi m_e}\right)^{1/2}, \quad (2)$$

with T_e, m_e, and m_i being the electron temperature, the electron mass, and the mass of the involved ion, respectively. For the most dominant ion in the system, H_3^+, $\Phi_w = -3.4T_e$. This means that $T_e \sim 0.7$–0.8 eV to have H_3^+ ions being accelerated to 2.5–3 eV. Although this value for T_e is a rough estimate that also depends on the applied sheath model, it indicates electron temperatures significantly higher than room temperature ($\sim 2.5 \times 10^{-2}$ eV).

To explain the presence of electrons with elevated temperatures, there must be a continued supply of energy to the system. Corresponding to the explanation for elevated mean ion energies in afterglows of inductively coupled H_2 plasmas,[30] this energy might be provided to the electrons by superelastic collisions with vibrationally excited hydrogen molecules. During the formation of the EUV-induced plasma (and in its early afterglow before the bulk of the electrons have cooled down to room temperature), H_2 molecules become excited by collisions with electrons. During a long period in the afterglow, even when the bulk of the electrons has cooled down to near room temperature, these long-living vibrational states give additional energy to superelastically colliding electrons and hence these can be pinpointed as the "system's battery."

With the current experimental data at hand, it is not possible to give a fully substantiated explanation for the fact that H_2^+ ions are detected such long after the gas was irradiated. However, this effect is most likely coupled to the elevated electron energies far in the afterglow phase. Apparently, taking into account the high loss rate of H_2^+ [see Eq. (1)], there must be a continued production term for H_2^+. Since the gas is irradiated with EUV photons only during the first 100 ns, production must be governed by other processes such as asymmetric charge transfer, electron impact dissociation of H_3^+ to H_2^+, and/or electron impact ionization. A global model of Mendez *et al.*[33] and simulations by van de Ven.[26] indicate that starting from $T_e \sim 1$ eV, the contribution of H_2^+ to the total ion density becomes larger with increasing electron temperature. However, more sophisticated modeling efforts for these conditions are needed to explain the observations in Fig. 3(b).

The findings of the current work [elevated electron energies for a considerable amount of time ($\sim$50 μs) after EUV irradiation] can only be fitted with earlier findings that the electron population thermalizes to room temperature on much shorter time scales (1–10 μs) when the electron energy distribution function (EEDF) has two components. In that case, the EEDF is made up by a thermal region around room temperature (governing the observed ambipolar flow) and a high energy

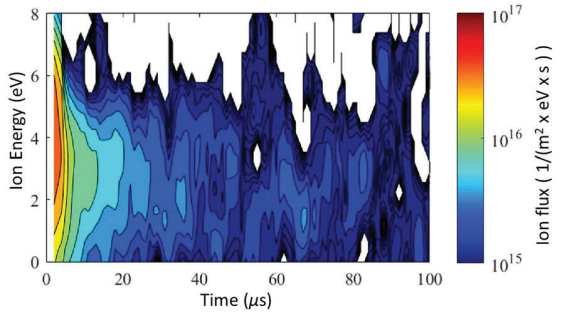

FIG. 3. Time-resolved IEDFs for the total ion flux from EUV-induced plasmas in pure H_2 gas at 5 Pa recorded by an RFEA.

tail determining the plasma potential with respect to its surroundings and, hence, the mean energy of the ions in the afterglow.

In conclusion, the results presented in this Letter are measurements of IEDFs of ions from EUV-induced plasmas that are temporally resolved. The main conclusions are that the ion energy unexpectedly remains high (a few electron-volts) for a considerably long time (tens of microseconds) after EUV irradiation of the gas and that—most likely coinciding with that—the contribution of H_2^+ to the total ion flux remains significant on much longer time scales (again tens of microseconds) than expected. These results provide more insight into the dynamics of EUV-induced plasmas and provide valuable input with respect to predicting and simulating the impact of EUV-induced plasma on EUV optical components.

The authors would like to acknowledge ASML for the financial support and measurement time on their EUV Source.

REFERENCES

[1] J. Benschop, V. Banine, S. Lok, and E. Loopstra, "Extreme ultraviolet lithography: Status and prospects," J. Vac. Sci. Technol., B **26**(6), 2204–2207 (2008).

[2] J. Beckers, T. van de Ven, R. van der Horst, D. Astakhov, and V. Banine, "EUV-induced plasma: A peculiar phenomenon of a modern lithographic technology," Appl. Sci. **9**(14), 2827 (2019).

[3] M. H. L. Van der Velden, W. J. M. Brok, J. J. A. M. Van der Mullen, and V. Y. Banine, "Kinetic simulation of an extreme ultraviolet radiation driven plasma near a multilayer mirror," J. Appl. Phys. **100**(7), 73303 (2006).

[4] A. S. Kuznetsov, R. W. E. Kruijs, M. A. Gleeson, K. Schmid, and F. Bijkerk, "Hydrogen interaction with EUVL-relevant optical materials," J. Surf. Invest. **4**(4), 563–566 (2010).

[5] A. S. Kuznetsov, M. A. Gleeson, and F. Bijkerk, "Ion effects in hydrogen-induced blistering of Mo/Si multilayers," J. Appl. Phys. **114**, 113507 (2013).

[6] R. A. J. M. Van den Bos, C. J. Lee, J. P. H. Benschop, and F. Bijkerk, "Blister formation in Mo/Si multilayered structures induced by hydrogen ions," J. Phys. D **50**(26), 265302 (2017).

[7] M. G. Pelizzo, A. J. Corso, P. Zuppella, D. L. Windt, and G. Mattei, "Stability of extreme ultraviolet multilayer coatings to low energy proton bombardment," Opt. Express **19**(16), 14838–14844 (2011).

[8] A. Dolgov, D. Lopaev, T. Rachimova, A. Kovalev, A. Vasil'eva, C. J. Lee, V. M. Krivtsun, O. Yakushev, and F. Bijkerk, "Comparison of H_2 and He carbon cleaning mechanisms in extreme ultraviolet induced and surface wave discharge plasmas," J. Phys. D **47**(6), 65205 (2014).

[9] A. Dolgov, D. Lopaev, C. J. Lee, E. Zoethout, V. Medvedev, O. Yakushev, and F. Bijkerk, "Characterization of carbon contamination under ion and hot atom bombardment in a tin-plasma extreme ultraviolet light source," Appl. Surf. Sci. **353**, 708–713 (2015).

[10] K. Boller, R. P. Haelbich, H. Hogrefe, W. Jark, and C. Kunz, "Investigation of carbon contamination of mirror surfaces exposed to synchrotron radiation," Nucl. Instrum. Methods Phys. Res. **208**(1-3), 273–279 (1983).

[11] A. Bartnik, W. Skrzeczanowski, P. Wachulak, I. Saber, H. Fiedorowicz, T. Fok, and Ł. Węgrzyński, "Low-temperature photoionized plasmas induced in Xe gas using an EUV source driven by nanosecond laser pulses," Laser Part. Beams **35**(1), 42–47 (2017).

[12] A. Bartnik, H. Fiedorowicz, P. Wachulak, and T. Fok, "Time-resolved measurements of extreme ultraviolet (EUV) emission, from EUV-induced He, Ne, and Ar plasmas," Laser Part. Beams **49–54**, 1–6 (2019).

[13] R. M. Van Der Horst, J. Beckers, E. A. Osorio, T. H. M. Van De Ven, and V. Y. Banine, "Radiating plasma species density distribution in EUV-induced plasma in argon: A spatiotemporal experimental study," Plasma Sources Sci. Technol. **24**(6), 065016 (2015).

[14] D. I. Astakhov, W. J. Goedheer, C. J. Lee, V. V. Ivanov, V. M. Krivtsun, K. N. Koshelev, D. V. Lopaev, R. M. Van Der Horst, J. Beckers, E. A. Osorio *et al.*, "Exploring the electron density in plasma induced by EUV radiation: II. Numerical studies in argon and hydrogen," J. Phys. D **49**(29), 295204 (2016).

[15] A. Abrikosov, V. Reshetnyak, D. Astakhov, A. Dolgov, O. Yakushev, D. Lopaev, and V. Krivtsun, "Numerical simulations based on probe measurements in EUV-induced hydrogen plasma," Plasma Sources Sci. Technol. **26**(4), 45011 (2017).

[16] D. I. Astakhov, W. J. Goedheer, C. J. Lee, V. V. Ivanov, V. M. Krivtsun, A. I. Zotovich, S. M. Zyryanov, D. V. Lopaev, and F. Bijkerk, "Plasma probe characteristics in low density hydrogen pulsed plasmas," Plasma Sources Sci. Technol. **24**(5), 55018 (2015).

[17] D. Astakhov, *Numerical Study of Extreme-Ultra-Violet Generated Plasmas in Hydrogen* (Universiteit Twente, The Netherlands, 2016).

[18] R. M. van der Horst, E. A. Osorio, V. Y. Banine, and J. Beckers, "The influence of the EUV spectrum on plasma induced by EUV radiation in argon and hydrogen gas," Plasma Sources Sci. Technol. **25**(1), 015012 (2016).

[19] R. M. Van Der Horst, J. Beckers, E. A. Osorio, D. I. Astakhov, W. J. Goedheer, C. J. Lee, V. V. Ivanov, V. M. Krivtsum, K. N. Koshelev, D. V. Lopaev *et al.*, "Exploring the electron density in plasma induced by EUV radiation: I. Experimental study in hydrogen," J. Phys. D **19**, 145203 (2016).

[20] R. M. Van Der Horst, J. Beckers, E. A. Osorio, and V. Y. Banine, "Dynamics of the spatial electron density distribution of EUV-induced plasmas," J. Phys. D **48**(43), 432001 (2015).

[21] J. Beckers, F. M. J. H. van de Wetering, B. Platier, M. A. W. van Ninhuijs, G. J. H. Brussaard, V. Y. Banine, and O. J. Luiten, "Mapping electron dynamics in highly transient {EUV} photon-induced plasmas: A novel diagnostic approach using multi-mode microwave cavity resonance spectroscopy," J. Phys. D **52**(3), 34004 (2018).

[22] R. M. Van Der Horst, J. Beckers, S. Nijdam, and G. M. W. Kroesen, "Exploring the temporally resolved electron density evolution in extreme ultra-violet induced plasmas," J. Phys. D **47**(30), 302001 (2014).

[23] R. M. Van Der Horst, J. Beckers, E. A. Osorio, and V. Y. Banine, "Exploring the electron density in plasmas induced by extreme ultraviolet radiation in argon," J. Phys. D **48**(28), 285203 (2015).

[24] J. Beckers, R. M. Van Der Horst, E. A. Osorio, G. M. W. Kroesen, and V. Y. Banine, "Thermalization of electrons in decaying extreme ultraviolet photons induced low pressure argon plasma," Plasma Sources Sci. Technol. **25**(3), 35010 (2016).

[25] T. H. M. Van De Ven, P. Reefman, C. A. De Meijere, R. M. Van Der Horst, M. Van Kampen, V. Y. Banine, and J. Beckers, "Ion energy distributions in highly transient EUV induced plasma in hydrogen," J. Appl. Phys. **123**(6), 063301 (2018).

[26] T. H. M. van de Ven, *Ion Fluxes Towards Surfaces Exposed to EUV-Induced Plasmas* (Eindhoven University of Technology, 2018).

[27] J. Beckers, T. H. M. de Ven, C. A. De Meijere, R. M. der Horst, M. Van Kampen, and V. Y. Banine, "Energy distribution functions for ions from pulsed EUV-induced plasmas in low pressure N_2-diluted H_2 gas," Appl. Phys. Lett. **114**(13), 133502 (2019).

[28] K. Bergmann, G. Schriever, O. Rosier, M. Müller, W. Neff, and R. Lebert, "Highly repetitive, extreme-ultraviolet radiation source based on a gas-discharge plasma," Appl. Opt. **38**(25), 5413–5417 (1999).

[29] R. M. Van der Horst, *Electron Dynamics in EUV-Induced Plasmas* (Eindhoven University of Technology, 2015).

[30] M. Osiac, T. Schwarz-Selinger, D. O'Connell, B. Heil, Z. L. Petrovic, M. M. Turner, T. Gans, and U. Czarnetzki, "Plasma boundary sheath in the afterglow of a pulsed inductively coupled {RF} plasma," Plasma Sources Sci. Technol. **16**(2), 355–363 (2007).

[31] T. Oka, "Interstellar H_3^+," Chem. Rev. **113**(12), 8738–8761 (2013).

[32] M. A. Lieberman and A. J. Lichtenberg, *Principles of Plasma Discharges and Materials Processing*, 2nd ed. (John Wiley & Sons, Inc., 2005).

[33] I. Méndez, F. J. Gordillo-Vázquez, V. J. Herrero, and I. Tanarro, "Atom and ion chemistry in low pressure hydrogen dc plasmas," J. Phys. Chem. A **110**(18), 6060–6066 (2006).